An RST Control Design Based on Interval Technique for Piezomicropositoning Systems with Rate-Dependent Hysteresis Nonlinearities

Micky Rakotondrabe and Mohammad Al Janaideh

***Abstract*— We propose a feedforward-feedback control of piezomicropositioning systems for precise positioning over different operating conditions. Such systems exhibit rate-dependent hysteresis nonlinearities and badly damped oscillations characteristics. First, we introduce a rate-dependent Prandtl-Ishlinskii inverse model for feedforward compensation of hysteresis. This yields to compensation that can be described with an uncertain linear model with disturbances. To model the uncertainties, we use intervals. Then we propose a new interval design for a RST structured feedback controller. The proposed method permits to satisfy prescribed performances. Simulation and experiments on a piezoelectric actuator are carried out and show the efficiency of the proposed controller.**

I. Introduction

Piezoelectric actuators are one of the most used actuators to develop precise positioning systems and to develop systems working at small scales. These actuators are used in microrobotics for micromanipulation and microassembly applications [1]. Despite the interesting properties of piezoelectric actuators, they are known to exhibit nonlinearities (hysteresis, creep) and badly damped oscillations in their responses. Many studies have therefore been reported regarding the control and the attenuation of these phenomena, including feedforward scheme, feedback, and feedforward-feedback control schemes. Feedforward is particularly of great interest in applications where using sensors is not possible due to the lack of space. In counterpart, feedforward is very sensitive to modeling uncertainties and to external dirturbances. On the other hand, feedback and feedforward-feedback can offer robustness against model uncertainties additionally to specified performances satisfaction. Over feedback control, feedforward-feedback is able to furnish supplementary performances that feedback alone would not be able to give [2].

In this paper, we suggest the design of a feedforward-feedback control for piezoelectric actuators. The feedforward is to compensate for the rate-dependent hysteresis of the actuators and the additional feedback is to ensure performances robustness and to reject possible disturbances.

There are numerous studies regarding the modeling of hysteresis in piezoelectric actuators but few of them are extended to feedforward control. The latters include: the Bouc-Wen approach [3], the Preisach approach [4], and the Prandtl-Ishlinskii approach [5], [6]. In the Prandtl-Ishlinskii approach, the rate-dependent Prandtl-Ishlinskii (RDPI) model is particularly able to approximate the hysteresis with shape changing versus the rate and versus the frequency of the driving input. In fact, much below the resonance frequency of many piezoelectric actuators, the hysteresis is observed to be yet rate-dependent. Taking into account such rate-dependency is essential in order to reduce modeling uncertainties and thus to increase the efficiency of a feedforward control scheme. This paper introduces first a RDPI model and its inverse to compensate for rate-dependent hysteresis in piezoelectric actuators. The compensation yields a linear model augmented with a bounded error that we will consider as an input disturbance. Then, the feedforward scheme is augmented with a feedback controller in order to ensure robustly certain prescribed performances. To that aim, a new design of the RST controller on the basis of interval techniques is proposed. The proposed RST controller is able to ensure *a priori* specified performances despite uncertain parameters in the linear model and despite input disturbance.

Interval techniques received many attention in estimation [7], and robotics control [8] Regarding feedback controllers for interval systems, various techniques have been studied: PID structure [9], [10], or controller based on performances inclusion design [11]. An advantage of using intervals to model uncertain parameters is the simplicity. The controllers design is generally a combination of the classical control tools with interval techniques. Relative to the above cited interval controllers design and the interval RST in [12], we propose a new RST controller that does not require solving inversion problem, which is therefore simpler.

II. RDPI feedforward controller

First the RDPI model is reminded. Then, the inverse of the model is given. Such inverse model is generally employed as feedforward controller, or compensator, for an actuator that exhibits a rate-dependent hysteresis.

M. Rakotondrabe is with Laboratoire Génie de Production, ENIT/Toulouse INP, Tarbes, France, mrakoton@enit.fr M. Al Janaideh is with the department of Mechanical Engineering, [2]Memorial University, St. John's, NL, Canada, maljanaideh@mun.ca. This work was supported by the CODETRACK project (ANR-17-CE05-0014-01) and France-Canada Mobility Funding for Researchers.

A. The model

Let $0 = t_0 < t_1 < \cdots < t_m$ be a partition of the interval $[0, T]$ such that v_r is monotone (nondecreasing or nonincreasing) in each interval $[t_{i-1}, t_i]$, $i = 1, \ldots, m$. A RDPI hysteresis model $\hat{\Phi}$ that approximates a real hysteresis Φ with input $v_r(t)$ and output $v(t)$ is defined as a superposition of n_h weighted rate-dependent play operators such that [13]

$$v(t) = \hat{\Phi}[u](t) = c_0 v_r(t) + \sum_{j=1}^{n_h} c_j \psi_{z_j(t)}, \tag{1}$$

where c_0 and c_j are the weights, $\psi_{z_j(t)}[v_r](t)$ is the rate-dependent play operator. Each play operator $\psi_{z_j(t)}$, with $j = 1, \cdots, n_h$, is characterized by a dynamic threshold $z_j(t)$ and is described for $t \in]t_i, t_{i-1}]$ with $\eta_j(t) = \psi_{z_j(t)}$ as

$$\eta_j(t) = \max\{v_r(t) - z_j(t), \min\{v_r(t) + z_j(t), \eta(t_{i-1})\}\}, \tag{2}$$

where $z_j(\dot{u}(t)) = \alpha j + \beta|\dot{u}(t)|$, where α and β are positive constant, and $v(0) = \max\{u(0) - r_j(0), \min\{u(0) + r_j(0), 0\}\}$.

B. The inverse model

The inverse of the RDPI model $\hat{\Phi}$ is denoted $\hat{\Phi}^{-1}$ and is called RDPI inverse model in the sequel. Its input is $v_r(t)$ and the output is $u(t)$. The output of the inverse RDPI model $u(t) = \hat{\Phi}^{-1}$can be expressed as

$$u(t) = g_0 v_r(t) + \sum_{j=1}^{n_h} g_j \psi_{s_j(t)}[v_r](t), \tag{3}$$

where $s_j(\dot{v}_r(t))$ are positive thresholds and g_0 and g_j are the weights of the inverse model. The dynamic threshold s_j and the weights g_0 and g_j are derived from the dynamic thresholds r_j and the weights c_0 and c_j [13]. We can write

$$v(t) = v_r(t) + b(t), \tag{4}$$

where $b(t)$ is the error of the compensation.

C. The new model

Eq. (4) provides a linear relation between the new input $v_r(s)$ and the output displacement $y(s)$ of the piezoelectric actuator. This relation is valid at frequencies lower than the resonance where the RDPI model is identified. To extend the model in order to account for the dynamics of the actuator, the Hammerstein structure is suggested. It consists in considering the actuator behavior as a cascade of a nonlinear part valid at low frequency and a linear dynamics. Hence Fig. (1-a) represents the Hammerstein scheme augmented with the RDPI inverse model. The actuator is represented here with the RDPI hysteresis model and a normalized linear dynamics $D(s)$, with $D(s = 0) = 1$. Considering Eq. (4), a new linear dynamical model $G(s) = kD(s)$ is therefore obtained as schemated in Fig. (1-b) where the input disturbance is: $d(s) = b(s)D(s)$.

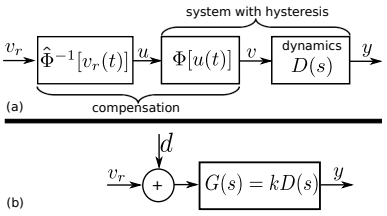

Fig. 1: (a) the compensation, and (b) the new system.

In many applications of piezoelectric actuators, a 2^{nd} order model is sufficient. It considers the bandwidth and first resonance while remaining simple. Thus, we take:

$$G(s) = k.D(s) = \frac{k}{\frac{1}{\omega_n^2}s^2 + \frac{2\zeta}{\omega_n}s + 1} \tag{5}$$

with ω_n the natural frequency and ζ the damping ratio. Due to the high sensitivity of miniaturized systems face to the environment however, their model parameters are uncertain [14]. Piezoelectric actuators are specifically very sensitive to temperature variation and to surrounding vibration. One way in the literature to model in an easy way such uncertainties in piezoelectric actuators models is intervals [15], [11]. Once an interval model is obtained, interval techniques can be combined with control techniques to synthesize a robust controller that will further ensure the stability and the performances of the closed-loop despite the uncertainties ranging in the intervals. Because of this easy way to bound uncertainties, we suggest to use interval models in this paper. Thus, "point" model in Eq. (5) becomes:

$$[G](s) = \frac{[k]}{\frac{1}{[\omega_n]^2}s^2 + \frac{2[\zeta]}{[\omega_n]}s + 1} = \frac{[k]}{[a_2]s^2 + [a_1]s + 1} \tag{6}$$

such that the static gain, the natural frequeny and the damping ratio of the actuator model are uncertain but within the intervals $[k]$, $[\omega_n]$ and $[\zeta]$, respectively.

III. An interval RST controller design

Having the interval model in Eq. (6) to approximate the behavior of the piezoelectric actuator with the RDPI inverse model, we propose to add a feedback controller in order to reject any disturbance, including the internal disturbance $d(s)$ due to compensation error, and to satisfy certain prescribed tracking performances. We propose here a RST controller feedback structure as it is known to be robust against disturbance additionally to its robustness to ensure static error deletion.

A. Structure

Let Fig. (2-a) (equivalently Fig. (2-b)) represent the new model augmented with a RST structured feedback controller. Despite the fact that RST controllers were originally and were systematically designed in the discrete-domain, we propose here a continuous-domain design combined with interval models. Therefore, R, S and T are polynomials in the Laplace variable s.
In the classical version, i.e. without using intervals, the basic idea of the RST controller is to find the polynomials

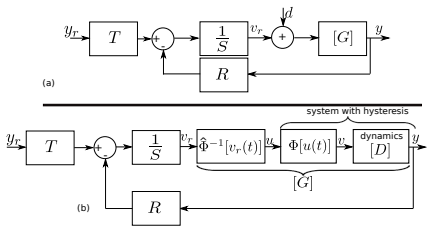

Fig. 2: (a): the RST controller applied to the new system. (b): details with the RDPI inverse model.

R, S and T such that the feedback in Fig. (2-a) has its poles equal to imposed/specified poles. This is why the RST approach is among the poles assignment approaches. The found controller will even reject an input disturbance d if certain conditions are satisfied during the design steps. Since we are dealing with intervals, we propose an interval RST controller design. In this case, the specifications are also intervals. One important result in interval techniques that will be used during the further design is the performances inclusion in interval transfer functions. This is reminded in Section- (III-B).

B. Performances inclusion for stable transfer functions

Performances inclusion in interval models has been used for controllers synthesis [11] and for actuators structures design [1]. We use it to design the RST feedback controller. The theorem contains one property for the frequency domain performances and one property for the time domain performances. Consider two stable interval systems having the same polynomials degrees m and n:

$$[H_1](s) = \frac{\sum_{l=0}^{m} [p_{1l}] \cdot s^l}{\sum_{k=0}^{n} [q_{1k}] \cdot s^k} \quad , \quad [H_2](s) = \frac{\sum_{l=0}^{m} [p_{2l}] \cdot s^l}{\sum_{k=0}^{n} [q_{2k}] \cdot s^k} \tag{7}$$

Theorem 3.1: Performances inclusion theorem [16].
In the frequency domain:

$$if \begin{cases} [q_{1k}] \subseteq [q_{2k}], \quad \forall k = 1 \cdots n \\ and \\ [p_{1l}] \subseteq [p_{2l}], \quad \forall l = 1 \cdots m \end{cases} \Rightarrow \begin{cases} [\rho]([H_1](j\omega)) \subseteq [\rho]([H_2](j\omega)) \\ and \\ [\varphi]([H_1](j\omega)) \subseteq [\varphi]([H_2](j\omega)) \end{cases}$$

In the time domain:

$$if \begin{cases} [q_{1k}] \subseteq [q_{2k}], \quad \forall k = 1 \cdots n \\ and \\ [p_{1l}] \subseteq [p_{2l}], \quad \forall l = 1 \cdots m \end{cases} \Rightarrow [h_1](t) \subseteq [h_2](t)$$

where $[\rho]([H_i](j\omega)$ is the set of magnitude of the interval system $[H_i]$, $[\varphi]([H_i](j\omega)$ is its argument and $[h_i](t)$ is the impulse response of the two systems.

As a definition, we say that $[H_1](s) \subseteq [H_2](s)$ when $[q_{1k}] \subseteq [q_{2k}]$ and $[p_{1l}] \subseteq [p_{2l}]$.

C. Problem formulation

Decompose $[G](s)$ as: $[G](s) = \frac{[B](s)}{[A](s)}$ with $[B](s) = [k]$ and $[A](s) = [a_2]s^2 + [a_1]s + 1$. From Fig. (2-a):

$$y(s) = \frac{[B]T}{([A]S + [B]R)} y_r(s) + \frac{[B]S}{([A]S + [B]R)} d(s). \tag{8}$$

Our target is to find the RST controller s.t. the controller reject the effect of the disturbance $d(s)$ and s.t. a desired tracking performance described by a desired closed-loop interval transfer function $[H_d](s)$ be satisfied. That is

- disturbance rejection: to ensure disturbance rejection, the transfer function that links $d(s)$ and $y(s)$ should contain at least one zero, i.e. $S(s)$ should be of the following structure:

$$S(s) = s^z S_z(s), \tag{9}$$

where $S_z(s)$ is a polynomial with a relative degree of z with regards to $S(s)$.

- tracking performance: according to the performances inclusion result in Theorem- (III-B), the following inclusion permits to the closed-loop to satisfy the desired specification described by $[H_d](s)$:

$$\frac{[B](s)T(s)}{([A](s)S(s) + [B](s)R(s))} \subseteq [H_d](s) \tag{10}$$

Indeed, Eq. (10) satisfies $y(s) \subseteq [H_d](s) y_r(s)$ and thus the output follows prescribed and desired evolution.

D. Rewriting the problem

Let us decompose the desired closed-loop transfer function as: $[H_d](s) = \frac{[B_m](s)}{[A_m](s)}$ where $[A_m](s)$ will be called interval reference polynomial. For existence of solution, $deg[A_m] \geq 2 \times deg[A]$. In the sequel we take: $deg[A_m] = 2 \times deg[A]$. Therefore, the above RST controller design problem becomes in finding the polynomials $R(s)$, $S(s)$ and $T(s)$ such that we satisfy the following conditions:

- condition-1: for disturbance rejection, let us consider that $S(s)$ exhibits one zero, i.e. $z = 1$. This is because we do not know the order of S at this time and because we will have more degrees of freedom in S by minimizing z. In counterpart, only low frequency disturbance will be rejected when the relative degree z is low. Because the disturbance d is due to error of hysteresis compensation that is supposed to be much below the resonance frequency, $z = 1$ is sufficient, i.e.:

$$S(s) = s.S_1(s) \tag{11}$$

- condition-2: from Inclusion. (10), we have:

$$[A](s)S(s) + [B](s)R(s) \subseteq [A_m](s) \tag{12}$$

Inclusion. (12) is an interval inclusion version of the Diophantine equation.

- condition-3: from Inclusion. (10), we also have:

$$[B](s)T(s) \subseteq [B_m](s) \tag{13}$$

- condition-4: finally, similarly to Diophantine equation [17], the Diophantine inclusion in Inclusion. (12) has unique solutions iff:

$$deg(R) = deg([A]) \tag{14}$$

Eq. (14) is to ensure that one has the same number of independent inclusions and of unknown variables.

Considering condition-1 ($S(s) = s.S_1(s)$) and the closed-loop transfer function $\frac{[B](s)T(s)}{([A](s)S(s)+[B](s)R(s))}$ however, the RST controller ensures a zero steady-state tracking performance error by taking:

$$T(s=0) = R(s=0) \tag{15}$$

Hence, the problem finally becomes:

Problem 3.1: Find the polynomials $R(s)$, $S(s)$ and $T(s)$ s.t.: (a) Robust disturbance rejection: $S(s) = s.S_1(s)$ (b) Tacking performances through Diophantine inclusion: $[A](s)S(s) + [B](s)R(s) \subseteq [A_m](s)$ (c) Numerator inclusion to complete the tracking performances: $[B](s)T(s) \subseteq [B_m](s)$ (d) Robust steady-state tracking performance: $T(s=0) = R(s=0)$ (e) Unicity of solution for the Diophantine inclusion: $deg(R) = deg([A])$.

Note that the disturbance rejection and the steady-state tracking performances are said robust here because they will be ensured independently to the model parameters. On the other hand, the transient part tracking performances are also said robust because, through the Diophante inclusion, the controller will ensure the specifications for any uncertainties of the model parameters described by intervals $[A](s)$ and $[B](s)$.

Because $[B](s) = [k]$ and because of condition-d of Problem. (3.1), we can keep $T(s)$ as a static gain for the sake of simplicity: $T(s) = R(s=0)$. Hence, $[B_m]$ is a static gain according to condition-c of Problem. (3.1). In this case, condition-c is not used to calculate any controller parameters since $R(s=0)$, and thus $T(s) = R(s=0)$ is already calculated from the Diophantine inclusion in condition-b. $[B_m]$ can be taken to be: $[B_m] = [k]R(s=0)$, which also satisfies condition-c and is thus defined *a posteriori* , i.e. once $R(s=0)$ is calculated.

E. Choice of the desired interval transfer function

The suggested RST interval controller design requires a desired interval transfer function $[H_d](s)$. This reference model is a transcription of the desired and specified tracking performances for the closed-loop. Let us take the following tracking performances specifications: (i) the settling time t_r of the closed-loop should be less or equal to t_{rmax}. Thus an interval desired settling time can be created as follows: $[t_r] = [0, t_{rmax}]$, and (ii) no oscillation is desired in the step-response. A first order system of type $\frac{1}{(\frac{[t_r]}{3}s+1)}$ can be a transcription of the above specifications. Taking into account the fact that $deg[A_m] = 2 \times deg[A] = 4$, the following structure is given for $[H_d](s)$:

$$[H_d](s) = \frac{[k]R(s=0)}{\left(\frac{[t_r]}{3}s+1\right)\left(\frac{[t_r]}{3n_f}s+1\right)^3} = \frac{[B_m](s)}{[A_m](s)} \tag{16}$$

where $n_f > 1$ is an integer to maintain the first order part $\frac{1}{(\frac{[t_r]}{3}s+1)}$ dominant. For that we take $n_f = 30$.

F. Resolution

The resolution of the RST controller is an iteration solving of the 5 conditions in Problem. (3.1), except condition-c. The iteration process is presented below. From condition-e, we impose

$$R(s) = \rho_2 s^2 + \rho_1 s + \rho_0, \tag{17}$$

where ρ_2, ρ_1 and $\rho_0 = R(s=0)$ are to be sought for. Then, because $deg([A_m]) = 4$, from the Diophantine equation in condition-b, we should have $deg(S) = 2$. Hence, considering condition-a, we impose

$$S(s) = s(\mu_1 s + \mu_0), \tag{18}$$

where μ_1 and μ_0 are to be sought for. Introducing Equ. (17) and Equ. (18) in the Diophantine inclusion in condition-b, we have

$$\begin{aligned}&\mu_1[a_2]s^4 + (\mu_1[a_1] + \mu_0[a_2])\,s^3 + (\mu_1 + \mu_0[a_1] + [k]\rho_2)\,s^2 \\ &+ (\mu_0 + [k]\rho_1)\,s + [k]\rho_0 \subseteq \tfrac{[t_r]^4}{81n_f^3}s^4 + \tfrac{[t_r]^3}{9n_f^2}\left(1+\tfrac{1}{3n_f}\right)s^3 \\ &+ \tfrac{[t_r]^2}{3n_f}\left(1+\tfrac{1}{n_f}\right)s^2 + \tfrac{[t_r]}{3}\left(1+\tfrac{1}{n_f}\right)s + 1\end{aligned} \tag{19}$$

Finally, from Inclusion. (19) and from condition-d, the RST controller parameters are therefore calculated to satisfy the following inclusions:

$$\begin{cases} \mu_1 \in \frac{[t_r]^4}{81n_f^3[a_2]}, \mu_0 \in \frac{1}{[a_2]}\left(\frac{[t_r]^3}{9n_f^2}\left(1+\frac{1}{3n_f}\right) - \mu_1[a_1]\right) \\ \rho_2 \in \frac{1}{[k]}\left(\frac{[t_r]^2}{3n_f}\left(1+\frac{1}{n_f}\right) - \mu_1 - \mu_0[a_1]\right) \\ \rho_1 \in \frac{1}{[k]}\left(\frac{[t_r]}{3}\left(1+\frac{1}{3n_f}\right) - \mu_0\right), \rho_0 \in \frac{1}{[k]}, T(s) = \rho_0 \end{cases} \tag{20}$$

As from Inclusion. (20), the derivation of the controller avoids set inversion problem and thus is straightforward in calculation.

G. The controller

Once the parameters of $R(s)$, $S(s)$ and $T(s)$ calculated, the controller is implemented. The scheme in Fig. (2) is not implementable because $T(s)$ and $R(s)$ are not causal. Instead, the scheme in Fig. (3) is used where $\frac{T(s)}{R(s)}$ is strictly causal and $\frac{R(s)}{S(s)}$ is causal non-strictly:

$$\frac{T(s)}{R(s)} = \frac{\rho_0}{\rho_2 s^2 + \rho_1 s + \rho_0}, \tag{21}$$

$$\frac{R(s)}{S(s)} = \frac{\rho_2 s^2 + \rho_1 s + \rho_0}{s(\mu_1 s + \mu_0)}. \tag{22}$$

IV. Experimental results

We apply the proposed interval RST controller design to a piezoelectric actuator in this section.

A. The experimental setup

The piezoelectric actuator to be used has a tubular structure. Piezoelectric tube actuators are the original actuator in atomic force microscopy (AFM) [18] for images scanning applications. Piezoelectric tube actuators can provide movement along x-axis, along y-axis and

along z-axis. In this paper, we only study the bending (displacement) along y-axis. The used experimental setup includes the piezoelectric actuator referenced as PT 230.94 from the *PI* company and which has $30mm$ of length and $3.2mm$ of external diameter. The internal diameter is $2.2mm$. The actuator voltage in this study will be ranging up to $\pm 100V$. A displacement sensor that measures the y bending at the tip of the piezotube actuator. The sensor principle is inductive and is the reference ECL202 from *LionPrecision* company. A computer from which the driving voltage is generated, the controller is implemented and the measurement is acquired. MATLAB-SIMULINK software is used for that. A dSPACE acquisition board, referenced as dS1104, serves as interface and contains the DAC (digital to analogic) and ADC (analogic to digital) converters. Since the voltage from the computer and the dSPACE acquisition board is limited to $\pm 10V$, a voltage amplifier with a gain of 20 is also used.

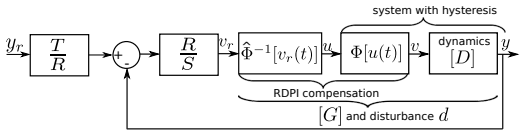

Fig. 3: Implementation of the RST and RDPI controllers.

B. Characterization and hysteresis compensation

The hysteresis of the piezoelectric actuator is displayed in Fig. (4), obtained at several frequencies ($1Hz$, $50Hz$, $150Hz$ and $200Hz$) much below the first resonance frequency which is approximately $778Hz$ (from the identified model in Eq. (23)). As from the hysteresis curves, the actuator exhibits rate-dependent hysteresis behavior.

A RDPI model $\hat{\Phi}[u(t)]$ was identified with the experimental data based on the four frequencies in Fig. (4). Then, an inverse RDPI model $u(t) = \hat{\Phi}^{-1}[v_r(t)]$ was derived and then put in cascade with the actuator as hysteresis compensator. Finally, the efficiency of the hysteresis compensator is tested with sine input signal $v_r(t)$ with frequencies from $1Hz$ to $200Hz$. Fig. (5) displays the results. They clearly show that, even for frequency that was not used for the identification, the compensation performance remains unchanged. The hysteresis is reduced from $\frac{8\mu m}{30\mu m} \approx 27\%$ (see $200Hz$ in Fig. (4)) to less than $\frac{1.5}{30} = 5\%$ (see $200Hz$ in Fig. (5)) while the average gain is unity ($v \approx v_r$). Then a step input $v_r = 15\mu m$ is applied to the actuator with hysteresis compensator. The normalized step response is shown in Fig. (6) (blue solid line) which reveals the badly damped oscillations property of the actuator. Such oscillations have to be attenuated by the further interval RST controller.

C. The new model

The linear model $G(s) = kD(s)$ in Eq. (5) is identified in this section. First the static gain k is identified from Fig. (5). Since this gain is approximately 1, we suggest to bound it with the following interval, such that any future uncertainty (for e.g. due to temperature variation) be accounted for: $[k] = [0.8\mu m, 1.2\mu m]$. Regarding the dynamics $D(s)$, its identification is made with the experimental step response in Fig. (6). The identified model is shown in Eq. (23) and its simulation is displayed in Fig. (6) (red dashed line) which indicates a good agreement with the experimental result. The obtained model is

$$D(s) = \frac{1}{41.83 \times 10^{-9} s^2 + 12.27 \times 10^{-6} s + 1} \tag{23}$$

To yield the interval model in Eq. (6), we take each parameter of Eq. (23) as center of the related interval parameter. The radius of each interval is taken as 20% of the center. The resulting interval parameters, listed in Eq. (24), are much larger than those in [15], [11] where the radius are 10%. Thus, the uncertainty considered in this paper is wider and the RST controller is more robust.

$$\begin{cases} [a_2] = [37.647 \times 10^{-9}, 46.013 \times 10^{-9}] \\ [a_1] = [11.043 \times 10^{-6}, 13.497 \times 10^{-6}], [k] = [0.8, 1.2] \end{cases} \tag{24}$$

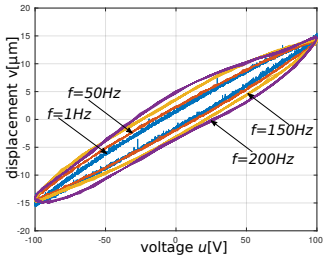

Fig. 4: Experimental hysteresis at different frequencies.

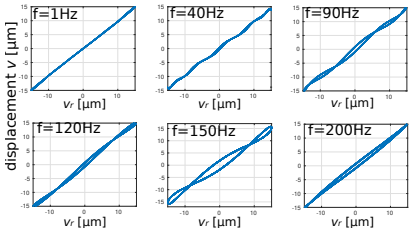

Fig. 5: Hysteresis compensation at different frequencies.

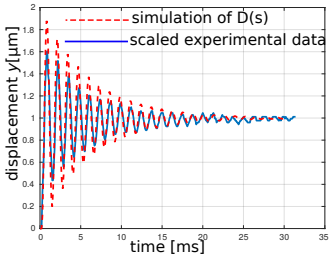

Fig. 6: Step response (actuator + RDPI inverse model).

D. Controller derivation and simulation

Specification used to create the reference model in Eq. (16) and to calculate the controller parameters is:

$t_{rmax} = 5ms$. Additionally to the oscillations to be damped, this will allow to reduce the settling time initially of $\approx 15ms$ (see Fig. (6)). The controller parameters are calculated using Inclusions. (20) and procedure in Section. (III-F). We obtain: $\mu_1 \in [0, 75.9 \times 10^{-9}]$. We select: $\mu_1 = 3.795 \times 10^{-9}$, $\mu_0 \in [-1.36 \times 10^{-6}, 0.41 \times 10{-}3]$. We select: $\mu_0 = 0.2 \times 10^{-3}$, $\rho_2 \in [0, 358 \times 10{-}9]$, $\rho_2 = 179 \times 10^{-9}$, $\rho_1 \in [0, 2.15 \times 10{-}3]$, $\rho_1 = 1.075 \times 10^{-3}$, $\rho_0 \in [0.833, 1.25]$,$\rho_0 = 1.04$. Finally, $T(s) = \rho_0 = 1.04$.Note that we selected the middle of each interval solution for each controller parameter but any values taken in the intervals will satisfy the specifications.

The designed RST controller is implemented and the closed-loop is simulated in Fig. (3). Thus, we apply the controller to the interval model $[G](s)$ with parameters in Eq. (24). The response y to a step reference input $y_r = 15\mu m$ is in Fig. (7-a) while the response y to a step disturbance $d = 1\mu m$ is in Fig. (7-b). They clearly reveal the efficiency of the closed-loop to satisfy the desired behavior (without oscillations, settling time $= 3.33ms$) and to reject the disturbance for any uncertainties within the interval model $[G](s)$.

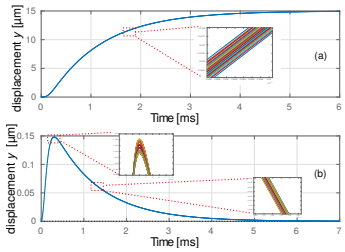

Fig. 7: Closed-loop simulation: (a) step response ($y_r = 15\mu m$), and (b) response to a disturbance of $d = 1\mu m$.

E. Experimental results of the closed-loop

We now apply the RST controller to the real piezoelectric tube actuator with its hysteresis compensator, still following the diagram in Fig. (3). The result is shown in Fig. (8) which presents a step response (reference is $y_r = 15\mu m$) without oscillations and with a settling time of $4ms$, and which demonstrate as well the efficiency of the proposed controller to satisfy the specifications.

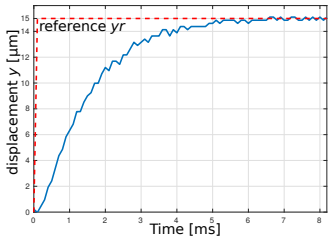

Fig. 8: Experimental step response of the closed-loop.

V. Conclusion

A feedforward-feedback controller design for piezoelectric actuators with hysteresis and badly damped oscillations was proposed. The feedforward controller was based on the RDPI approach in order to reduce rate-dependent hysteresis of the actuator. Then a RST controller structure was introduced for the feedback and a new interval design was proposed to this. The proposed controller design did not use set inversion problem, which eased the controller parameters calculation. Both simulation and experiments were carried out which shown the efficiency of the proposed control design.

References

[1] M. Rakotondrabe, M. Janaideh, A. Bienaim, and Q. Xu, "Smart materials-based actuators at the micro/nano-scale," *Characterization, Control and Applications.*, 2013.

[2] S. Devasia, E. Eleftheriou, and S. R. Moheimani, "A survey of control issues in nanopositioning," *IEEE Transactions on Control Systems Technology*, vol. 15, no. 5, pp. 802–823, 2007.

[3] M. Rakotondrabe, "Bouc–wen modeling and inverse multiplicative structure to compensate hysteresis nonlinearity in piezoelectric actuators," *IEEE Transactions on Automation Science and Engineering*, vol. 8, no. 2, pp. 428–431, 2010.

[4] X. Tan and J. S. Baras, "Modeling and control of hysteresis in magnetostrictive actuators," *Automatica*, vol. 40, no. 9, pp. 1469–1480, 2004.

[5] M. Rakotondrabe, "Multivariable classical prandtl–ishlinskii hysteresis modeling and compensation and sensorless control of a nonlinear 2-dof piezoactuator," *Nonlinear Dynamics*, vol. 89, no. 1, pp. 481–499, 2017.

[6] M. Al Janaideh and M. Rakotondrabe, "Control of piezoelectric positioning systems using inverse rate-dependent prandtl-ishlinskii model and performances inclusion based interval techniques," *Mathematical Modelling of Natural Phenomena*, vol. xx, no. x, 2019.

[7] M. Kieffer and E. Walter, "Guaranteed estimation of the parameters of nonlinear continuous-time models: Contributions of interval analysis," *International Journal of Adaptive Control and Signal Processing*, vol. 25, no. 3, pp. 191–207, 2011.

[8] B. Desrochers and L. Jaulin, "Computing a guaranteed approximation of the zone explored by a robot," *IEEE Transactions on Automatic Control*, vol. 62, no. 1, pp. 425–430, 2016.

[9] J. Bondia, A. Kieffer, E. Walter, J. Monreal, and J. Pico, "Guaranteed tuning of pid controllers for parametric uncertain systems," in *43rd IEEE Conference on Decision and Control (CDC)*, vol. 3, 2004, pp. 2948–2953.

[10] S. Khadraoui, M. Rakotondrabe, and P. Lutz, "Combining hâĹđ approach and interval tools to design a low order and robust controller for systems with parametric uncertainties: application to piezoelectric actuators," *International Journal of control*, vol. 85, no. 3, pp. 251–259, 2012.

[11] ——, "Interval modeling and robust control of piezoelectric microactuators," *IEEE Transactions on Control Systems Technology*, vol. 20, no. 2, pp. 486–494, 2011.

[12] ——, "Design of rst-structured controller for parametric uncertain system using interval analysis: application to piezocantilever," *Asian J. Control*, vol. 15, no. 1, pp. 142–154, 2013.

[13] M. Al Janaideh and P. Krejčí, "Inverse rate-dependent prandtl–ishlinskii model for feedforward compensation of hysteresis in a piezomicropositioning actuator," *IEEE/ASME Transactions on mechatronics*, vol. 18, no. 5, pp. 1498–1507, 2012.

[14] M. Rakotondrabe, Y. Haddab, and P. Lutz, "Quadrilateral modelling and robust control of a nonlinear piezoelectric cantilever," *IEEE Transactions on Control Systems Technology*, vol. 17, no. 3, pp. 528–539, 2008.

[15] M. Hammouche, A. Mohand-Ousaid, P. Lutz, and M. Rakotondrabe, "Robust interval luenberger observer-based state feedback control: Application to a multi-dof micropositioner," *IEEE Transactions on Control Systems Technology*, 2018.

[16] M. Rakotondrabe, "Performances inclusion for stable interval systems," in *American Control Conference (ACC)*, 2011, pp. 4367–4372.

[17] H. Bourlès and G. K. Kwan, *Linear systems*. John Wiley & Sons, 2013.

[18] G. Binnig, C. F. Quate, and C. Gerber, "Atomic force microscope," *Physical review letters*, vol. 56, no. 9, p. 930, 1986.